Neural Computing and Applications (2020) 32:9093–9111
https://doi.org/10.1007/s00521-019-04420-5

ORIGINAL ARTICLE

Microgrid management using hybrid inverter fuzzy-based control

Mustapha Habib[1] · Ahmed Amine Ladjici[1] · Abdelghani Harrag[2,3]

Received: 22 June 2019 / Accepted: 7 August 2019 / Published online: 13 August 2019

Abstract

Microgrid systems are becoming a very promising solution to meet the power demand growth especially in remote areas where diesel generators (DG) are commonly used as a main energy source. Photovoltaic (PV) systems are commonly used as a sustainable energy source to economize DG fuel. Due to the intermittent and fluctuating behavior of PV generators, energy storage systems (ESS) such as electrochemical battery are suggested. PV and ESS are usually connected using one inverter/charger called hybrid inverter. The power management is crucial to optimize the fuel consumption and operate efficiently ESS. Additionally, in an off-grid operation, the microgrid frequency becomes sensible due to the slow dynamic of DG which requires an additional control tool to improve the frequency regulation. This paper proposes a new power management based on Mamdani fuzzy logic. The proposed controller considers the targets mentioned above by only controlling the hybrid inverter. Simulation results prove that fuzzy-based controller reduces the DG fuel consumption by more than 12% compared to classical hysteresis management control. Moreover, the proposed controller performs efficiently regarding the conventional frequency regulation, which is widely used in microgrid control.

Keywords Diesel generator · DG · Photovoltaic · PV · Electrochemical battery · Power management · Mamdani fuzzy logic

List of symbols

I_{ph}	Photocurrent
I	Diode saturation current
q	Coulomb constant (1.602×10^{-19} C)
K	Boltzmann's constant (1.38×10^{-23} J/K)
T	Cell temperature
PN	P–N junction ideality factor
R_s	Intrinsic series resistance
R_{sh}	Intrinsic parallel resistance
S	Real solar radiation
S_{ref}	Solar radiation in standard test conditions (1000 w/m^2)
T_{ref}	Cell absolute temperature in standard test conditions
$I_{ph\text{-}ref}$	Photocurrent in standard test conditions
C_T	Temperature coefficient
$I_{s\text{-}ref}$	Diode saturation current in standard test conditions
E_g	Band-gap energy of the cell semiconductor
E	Battery no-load voltage
E_o	Battery constant voltage
k	Polarization voltage
Q	Battery capacity
A	Exponential zone amplitude
B	Exponential zone time constant inverse
E_{full}	Fully charged voltage
E_{exp}	Voltage at the end of exponential zone
Q_{exp}	Charge at the end of exponential zone
E_{nom}	Voltage at the end of nominal zone
Q_{nom}	Charge at the end of nominal zone
F_{min}	Minimum allowed frequency value
F_r	Regulation frequency value
F_{max}	Maximum allowed frequency value
T_{sm}	Governor time constant
T_d	Engine time constant
R	Frequency drop
V_f	Excitation voltage of the synchronous machine

Abbreviations

MPPT	Maximum power point tracking
P&O	Perturb and observe

✉ Abdelghani Harrag
a.harrag@univ-setif.dz

[1] Departement of Electrical Engineering, USTHB, Algiers, Algeria

[2] Optics and Precision Mechanics Institute, Ferhat Abbas University, Cite Maabouda (ex. Travaux), 19000 Setif, Algeria

[3] CCNS Laboratory, Electronics Department, Faculty of Technology, Ferhat Abbas University, Campus Maabouda, 19000 Setif, Algeria

PV	Photovoltaic
SOC	State of charge
ESS	Energy storage system
PM	Power management
MG	Microgrid
FL	Fuzzy logic
DC	Direct current
AC	Alternative current
DG	Diesel generator

1 Introduction

In recent years, the demand for energy in remote areas is on the increase. To meet this ever-growing demand, energy is supplied using diesel generators (DG) in the framework of off-grid microgrid (MG). However, the production cost of such energy is relatively high; besides, there is a worldwide concern to reduce CO_2 emissions being the main cause of global warming. To face these challenges, photovoltaic (PV) systems were introduced and soon became extensively used. With a well-dimensioned PV system, the use of DG fuel can be dramatically decreased. Though, an efficient power management (PM) policy is required to optimally drive any possible energy storage system (ESS) such as electrochemical batteries [1–7].

PV power fluctuations, which depend highly on weather conditions, push the stability of MG in terms of frequency regulation to the limit. The stochastic nature of power demand can also have an additional effect. Since it is considered as a direct sign of power equilibrium between generation and consumption, frequency deviation from the rated value can reduce the reliability of connected equipment or even damage them. This is probable even when ESS is included due to the fast behavior of insolation fluctuations compared to DG and ESS dynamics. Many works have been proposed to solve such problem [8–14]; however, simultaneous targeting of MG energy management as a long horizon (hours) with MG frequency regulation as a short horizon (seconds) in one unique controller is a challenging task.

In Ref. [15], authors propose a hierarchical energy management strategy for an island PV/fuel cell/battery hybrid DC microgrid where the optimum structure and sizing scheme composed of PV generator, a battery, a fuel cell (FC) system and an electrolyzer are designed using HOMER pro-software. The proposed hierarchical energy management strategy is based on local control layer which is used to control the inherent operating characteristics; while the power flow between the battery and FC is allocated to minimize the hydrogen consumption using a system control layer. The proposed strategy has been tested and validated on an island DC MG hardware-in-loop Simulink platform established using RT-LAB real-time simulator.

In Ref. [16], authors proposed an adaptive supervisory energy management system to monitor, control, and optimize the performance of the hybrid FC/ESS power system. The proposed approach uses the adaptive Pontryagin's minimum principle (A-PMP) to adapt the control parameters using the state of charge (SOC) and load power feedback. The proposed method has been investigated using three different load profiles under MATLAB/Simulink environment as well as on experimental platform.

In Ref. [17], authors propose an optimized energy management system of hybrid system composed of FC and gas micro-turbines as backup sources and PV and wind as renewable energy sources. The proposed system uses neural network as well as fuzzy logic controllers in order to minimize the energy production cost and keeping buffer role of the hybrid power system. The proposed approach has been tested and validated using MATLAB/Simulink software for the overall hybrid system during 24-h load variation, proving the performance of the proposed control approach avoiding the problems of unexpected load peaks and/or discontinuous energy production.

In all previous studies, different controllers to manage and supervise MG within different control layers are developed and validated. Those layers are connected to each other, in which the higher layer (PM) manages the power of energy sources and storage in MG based on some economical and technical requirements, while the lower layer (power control) makes sure that the different subsystems follow the sent power references, usually via PI (proportional–integral) controllers. The purpose of this study is to combine power management and power control layers in one structure using fuzzy logic topology, this new control scheme will be able to manage different timescale tasks in MG from few seconds up to 1 day. The proposed FL controller has three objectives, namely DG fuel reduction, ESS SOC supervising, and MG frequency regulation. Various engineering applications of these days include FL to solve some technical problems [18–20].

Most of the industrial processes today are characterized by complex multivariable models which makes it hard—sometimes impossible—to use linear controllers. With appropriate logic rules, which should be grounded on a skilled human logic, FL controller can easily and robustly link between inputs and outputs to accomplish regulation, tracking or supervising tasks with only IF–THEN procedure. In the case of control/management, FL can accomplish several missions like optimal power sharing in a hybrid car [21], extracting the maximum of available power in a PV system [22, 23], or optimally manage the power flow in a MG [24]. In Refs [25, 26], similar

approaches to the one proposed here have been presented; however, the developed controllers have not been configured when ESS is connected; moreover, they aim just to find a trade-off between maximizing the PV production while controlling the frequency deviation, hence, a real power dispatching between DG, PV, load, and any possible ESS has not been treated.

As mentioned earlier, and unlike previously declared approaches, the contribution of the proposed method is to deal with different targets in different timescales using one controller, which are the DG fuel economy as a long-term management (up to 1 day); SOC supervising as a medium-term management (up to hours) and frequency control as a short-term management (up to seconds). Considering the different situations, FL gives high flexibility, robustness, and performance when applying control.

The remainder of this paper is organized as follows: In Sect. 2, mathematical modeling of MG components, that will be later simulated using the proposed method, is presented. Section 3 explains the topology of MG with the chosen control methods. Section 4 includes the hysteresis PM with conventional frequency regulation as a reference method as well as the proposed FL-based method. Computer simulation performed using the proposed method including an evaluation study versus the reference one is given in Sect. 5. Finally, Sect. 6 states the main conclusions of this work.

2 Modeling of energy sources and storage

In this section, mathematical models for MG components (DG, PV, and ESS) are detailed and simulated. No improvements have been added, since the main goal of this study is to contribute only in MG control and management.

2.1 Diesel generator model

A standard simplified model of DG and speed governor is illustrated in block diagram form (Fig. 1).

This model is widely used and perfectly describes the dynamic behavior of small diesel generator sets, as shown in [27]. The diesel engine and the valve actuator servomechanism are represented by first-order lags, with time constants T_d and T_{sm}, respectively (Fig. 2).

Parameters of the speed governor are the drop R and the proportional–integral regulator parameters. The objective of the PI control is to eliminate the steady-state frequency error, and in many cases (particularly in small and older units), it may be absent.

The diesel engine must be able to follow the variation in loads power. The frequency control performance indicates how well the diesel and its governor maintain the balance of active power in the system, whereas variation in voltage shows how well the gen-set and its voltage regulator maintain the balance of reactive power via the generator excitation (Fig. 3). Basically, frequency and voltage are not perfectly constants because the load power, and consequently the MG power balance, fluctuates continuously.

Thereafter, a numeric simulation with MATLAB/Simulink has been realized for DG for a 10-min scenario. The main parameters of diesel engine model are cited in Table 1.

The load power, diesel mechanical power, and voltage excitation variations are presented in Figs. 4, 5, and 6, respectively.

Figures 7 and 8 illustrate the DG produced power quality in terms of voltage and current (with no connected PV or ESS).

2.1.1 PV array model

PV cell is the most basic generation part in PV system. Single-diode mathematic model is applicable to simulate silicon PV cells which consist of a photocurrent source I_{ph}, a nonlinear diode, internal resistances R_s and R_{sh}. The mathematic relationship for the current and voltage in the single-diode equivalent circuit can be described as:

$$I = I_{ph} - I_s\left(e^{q\frac{V - I\cdot R_s}{PN\cdot K\cdot T}} - 1\right) - \frac{V - I\cdot R_s}{R_{sh}} \quad (1)$$

where I_{ph} is photocurrent; I is diode saturation current; q is coulomb constant (1.602×10^{-19} C); K is Boltzmann's constant (1.38×10^{-23} J/K); T is cell temperature (K); PN is P–N junction ideality factor; R_s and R_{sh} are intrinsic series and parallel resistances.

The photocurrent is the function of solar radiation and cell temperature, described as:

$$I_{ph} = \left(\frac{S}{S_{ref}}\right)\left[I_{ph-ref} + C_T(T - T_{ref})\right] \quad (2)$$

where S is the real solar radiation (W/m^2); S_{ref}, T_{ref} et $I_{ph\text{-}ref}$ are the solar radiation, cell absolute temperature and photocurrent in standard test conditions respectively; C_T is the temperature coefficient (A/K).

The diode saturation current varies with the cell temperature:

$$I_s = I_{s-ref}\left(\frac{T}{T_{ref}}\right)^3 e^{\left[\frac{qE_g}{PN\cdot K}\left(\frac{1}{T_{ref}} - \frac{1}{T}\right)\right]} \quad (3)$$

where $I_{s\text{-}ref}$ is the diode saturation current in standard test conditions; E_g is the band-gap energy of the cell semiconductor (eV), depending on the cell material.

The main physical parameters of the used PV array are cited in Table 2.

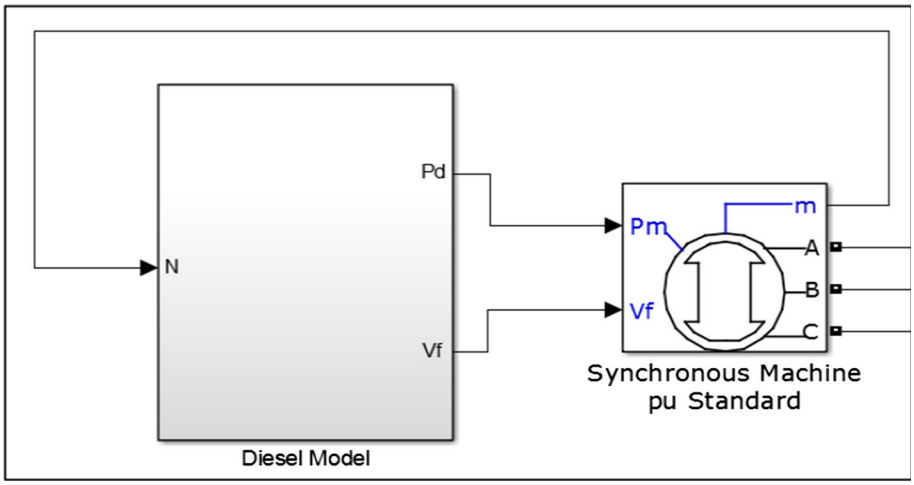

Fig. 1 DG model with MATLAB/Simulink

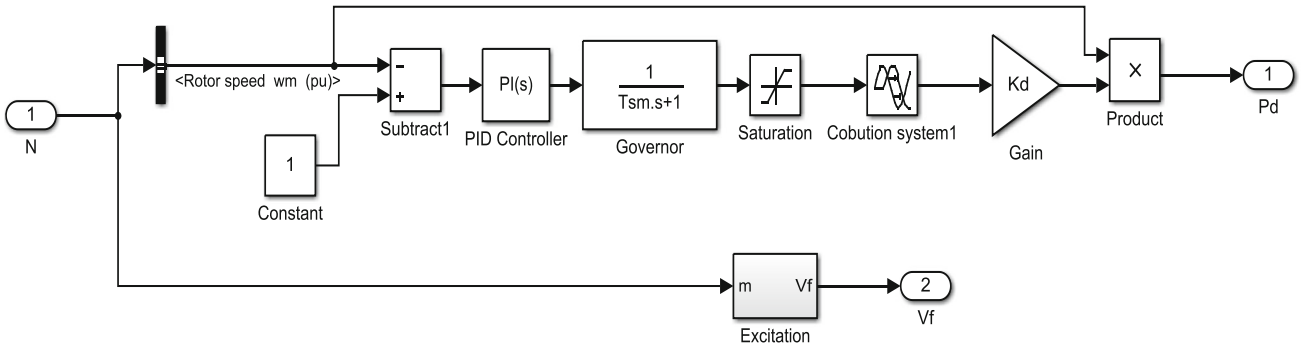

Fig. 2 Diesel engine model and the excitation system with Simulink

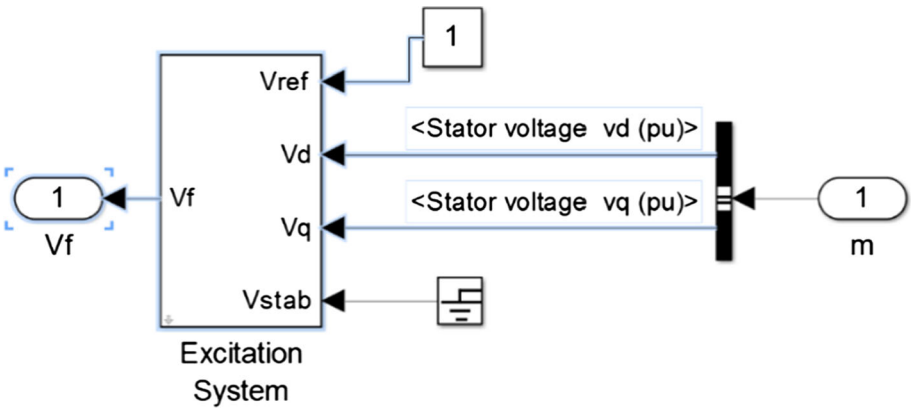

Fig. 3 Excitation system with Simulink

2.1.2 Battery model

The equivalent circuit for ESS model is the most suitable for dynamic simulation. Based on Shephred battery model, Ref. [28] presents a generic battery model for dynamic simulation, which assumes that the battery is composed of a controlled-voltage source with series resistance. The equivalent electric circuit is presented in Fig. 9.

The expression of the controlled-voltage source is:

$$E = E_0 - k\frac{Q}{Q - \int i_b \mathrm{d}t} + Ae^{-B\int i_b \mathrm{d}t} \quad (4)$$

where E is no-load voltage (V); E_0 is battery constant voltage (V); k is polarization voltage (V); Q is battery capacity (Ah); A is exponential zone amplitude (V); B is exponential zone time constant inverse (Ah^{-1}).

This model assumes that the internal resistance of the battery is kept constant during both charging and discharging cycles. All parameters are deduced from the

Table 1 Diesel model parameters

Parameters	Values
Nominal power (kVA)	250
Nominal voltage (V RMS)	400
Nominal rotor speed (RPM)	1500
Frequency (Hz)	50
Governor time constant T_{sm} (s)	0.2
Engine time constant T_d (s)	5
Combustion time delay (s)	0.2
Frequency drop R (Hz/pu)	2.5

discharging profile. Figure 10 shows the discharging characteristics of the battery at different currents.

All parameters can be calculated by three points marked on the figure, namely fully charged voltage (E_{full}), end of exponential zone (E_{exp}, Q_{exp}), and end of nominal zone (E_{nom}, Q_{nom}) (Table 3).

Formulas for calculating the model parameters are:

$$\begin{cases} A = E_{full} - E_{exp} \\ B = {}^{3}/_{Q_{exp}} \\ K = [E_{full} - E_{nom} + A(e^{-BQ_{nom}} - 1)] \end{cases} \quad (5)$$

3 Power topology and control

Figure 11 shows a whole MG system architecture.

The MG system is composed of a large PV array connected with two power-conditioning stages:

- DC/DC boost converter to rise up PV voltage and extract the maximum of available PV power thanks to maximum power point tracking (MPPT) technique;

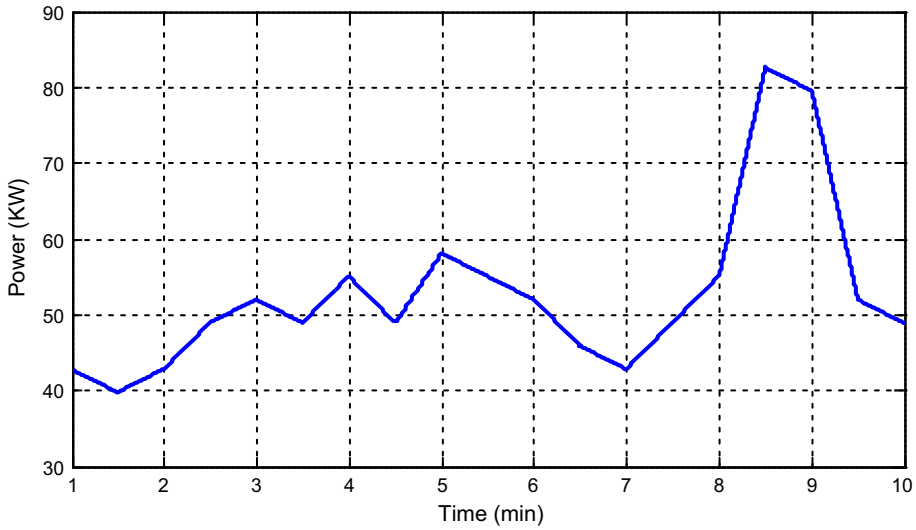

Fig. 4 Load power variation

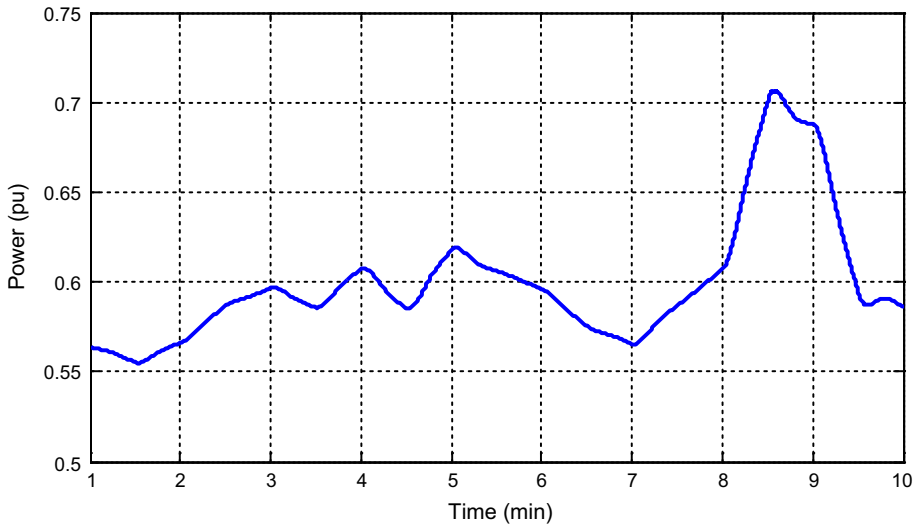

Fig. 5 Diesel mechanical power variation

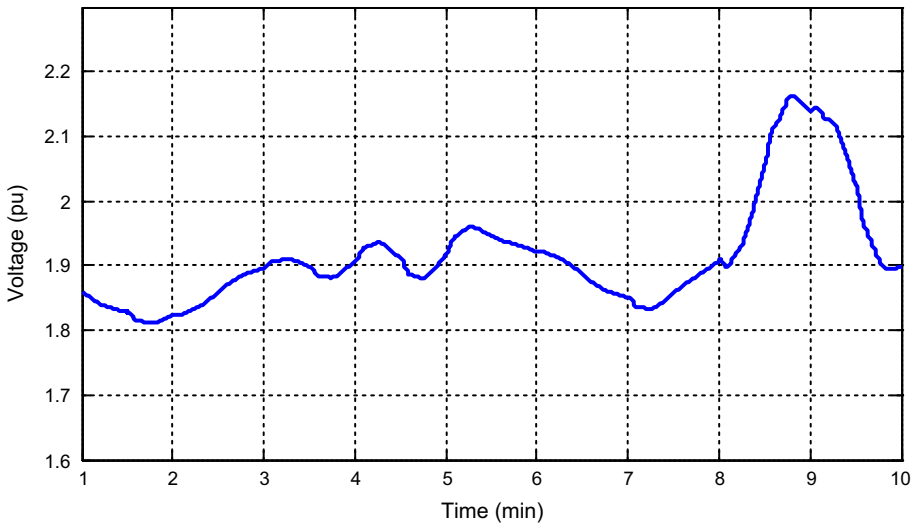

Fig. 6 DC excitation voltage variation

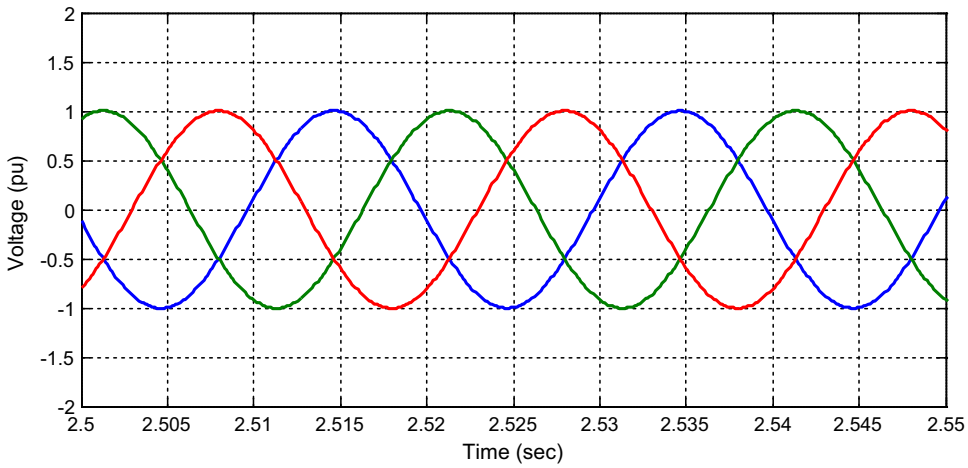

Fig. 7 AC voltage with only diesel generator

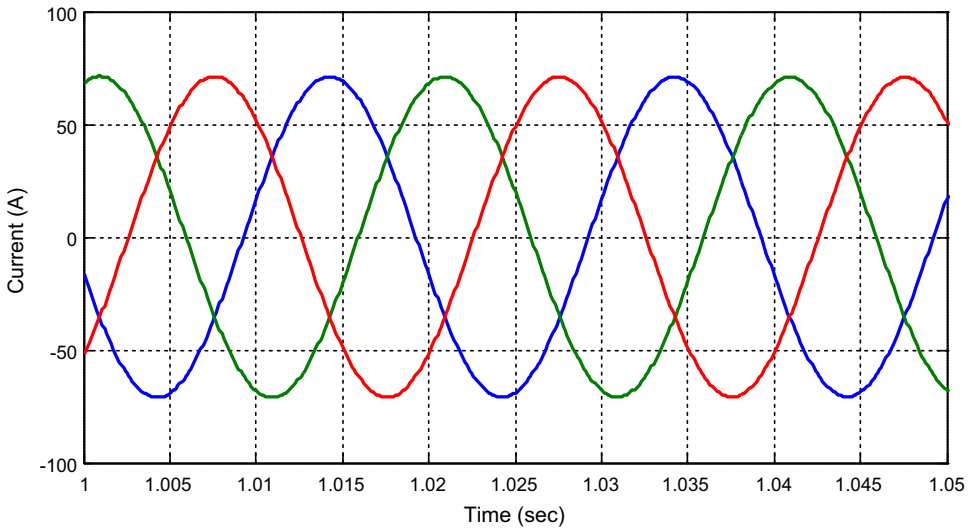

Fig. 8 AC current with only diesel generator

Table 2 PV model parameters

Parameters	Values
Cell	
Referenced solar irradiation S_{ref} (W/m^2)	1000
Referenced cell temperature T_{ref} (K)	298
Photocurrent at the standard conditions $I_{ph\text{-}ref}$ (A)	3.35
Band-gap energy E_g (eV)	1.237
Cell internal resistance R_s (Ω)	0.312
P–N junction ideality factor *A*	54
Temperature coefficient C_T (%)	0.065
Module	
Rated power (W)	220
Open-circuit voltage (V)	42
MPP voltage (V)	35
Short-circuit current (A)	7.23
MPP current (A)	6.90
Number of cells in the module	60
Array	
Parallel numbers of PV modules N_p	20
Series numbers of PV modules N_s	10
Rated power (kW)	44

- The second stage is DC/AC two-level PWM inverter/charger to convert DC current to AC current synchronized with MG;
- An additional ESS is connected to the DC side of PV inverter through reversible DC/DC buck–boost converter. The ESS DC-coupled topology is chosen since it does not require high complex control and synchronization procedures as AC-coupled one. Various power topologies for hybrid MG with different advantages are clarified in [29].

The addition of ESS gives more autonomy to the hybrid system which makes PV inverter connected to MG even when there is no available PV power (typically during nights or cloudy periods). However, ESS SOC must be permanently supervised and operated within two control limits; fully charged batteries cannot recover sudden PV excess which may then damage them, when frequent deep discharging may well reduce their operational lifetime.

ESS converter is controlled to keep DC voltage at the desired level. The hybrid inverter is controlled to exchange power with MG according to the set point sent manually from the MG operator or automatically from PM layer. In this work, the possibility to manage the power flow in MG by merely controlling the hybrid inverter has been proven, and this will be the main objective of Sects. 3 and 4.

3.1 Inverter control

The active and reactive powers are controlled separately with the help of PWM voltage-controlled inverter. The active power is controlled through the shifting angle φ between MG and inverter voltages using PI controller. The reactive power is controllable using the index modulation, and it is maintained at 1 permanently due to the fact that no need for additional voltage regulation, and consequently, no reactive power exchange is proposed in this work (Fig. 12). The MG voltage is maintained constant only with DG excitation system.

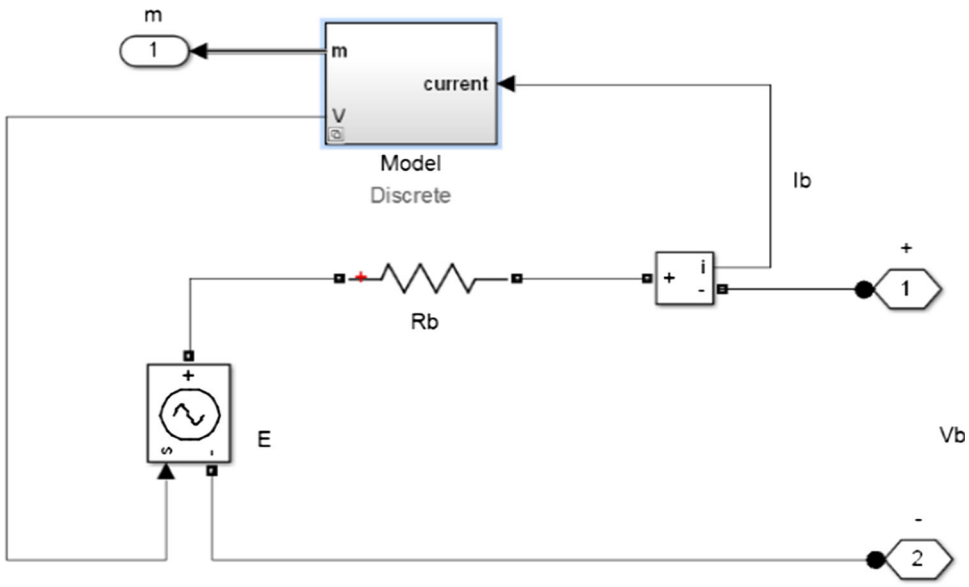

Fig. 9 Generic battery model with Simulink

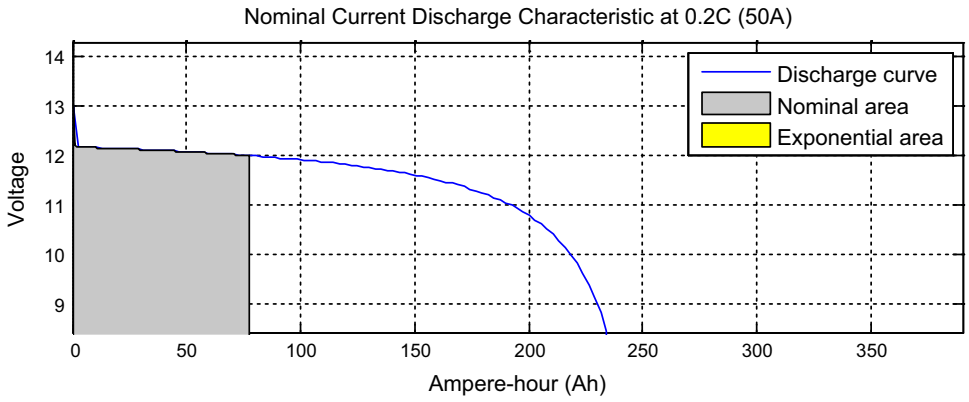

(a)

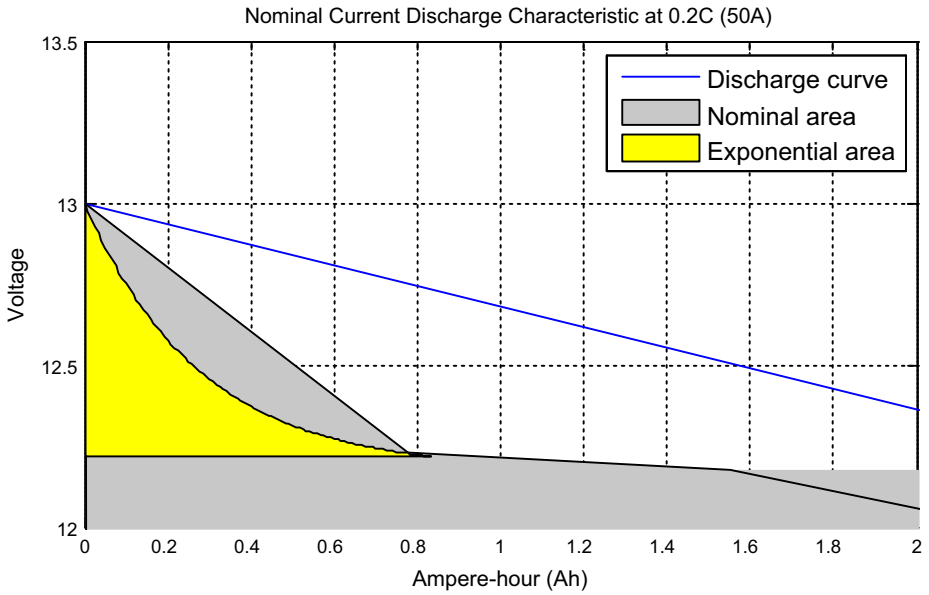

(b)

Fig. 10 **a** Characteristics curve of one lead acid cell at different discharge currents, **b** zoom-in of interval [0; 2 Ah]

3.2 Battery control

The DC/DC batteries converter is controlled in order to regulate the DC link voltage at a level in which the inverter can operate properly (700 V). This is feasible using two PI controllers within two combined control loops: the outer loop for voltage control which gives the reference to the inner one: current control. The entire Simulink-based diagram is represented in Fig. 13.

Table 3 ESS model parameters

Parameters	Values
Cell	
Fully charged voltage E_{full} (V)	13.06
End of exponential zone E_{exp} (V)–Q_{exp} (Ah)	12.21–0.83
Rated capacity C (Ah)	250
Rated voltage (V)	12
End of nominal zone E_{nom} (V)–Q_{nom} (Ah)	11.86–77.5
Nominal discharge current (A)	50
Internal resistance (mΩ)	4.8
Stack	
Number of cells on series	30
Number of cells on parallel	1
Rated power (kW)	30

3.3 MPPT control

The PV array is controlled to extract the maximum available power via MPPT. In this work, a simple P&O MPPT tool is chosen to select the PV current reference according to the MPP which depends essentially on solar irradiation (Fig. 14).

4 Power management

4.1 Hysteresis-based PM

The hysteresis-based PM consists of sending two power references (P_{min} and P_{max}) to the hybrid inverter according to two ESS SOC limits (SOC_{min} and SOC_{max}) (Fig. 15).

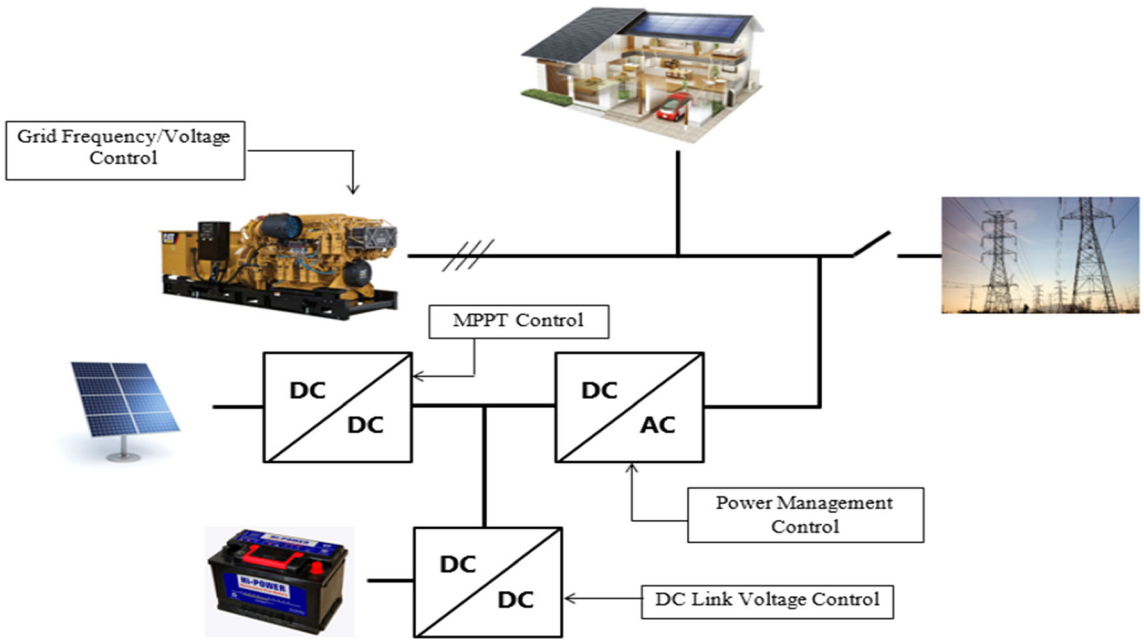

Fig. 11 Grid-connected hybrid power system

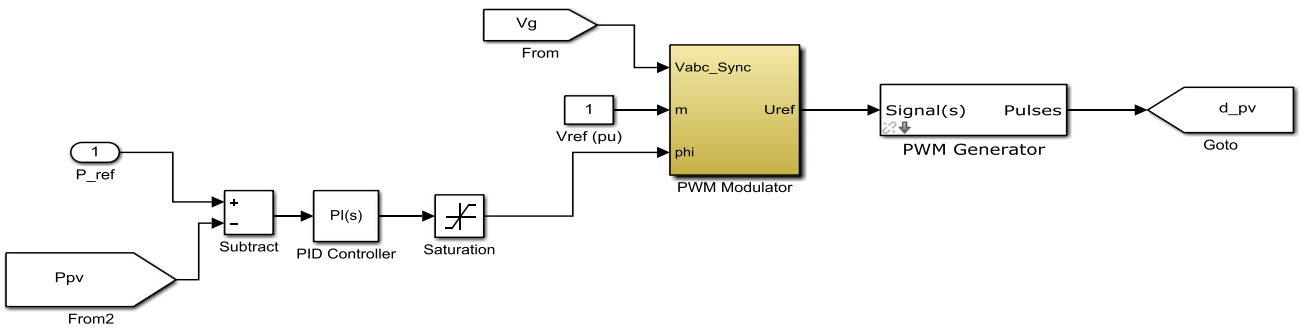

Fig. 12 Inverter/charger Simulink diagram control

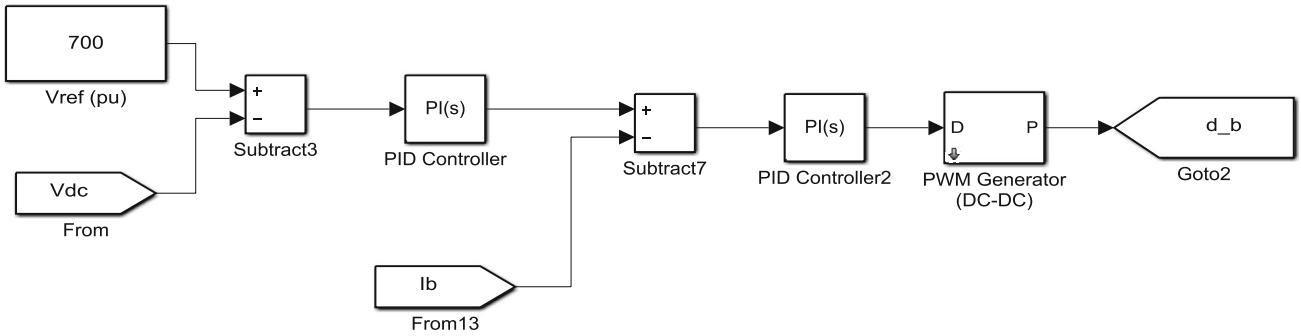

Fig. 13 ESS DC/DC converter control

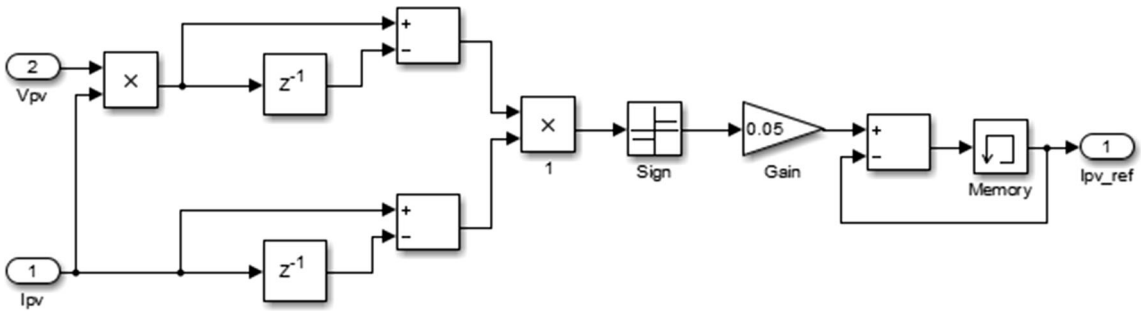

Fig. 14 Simulink-based P&O MPPT control

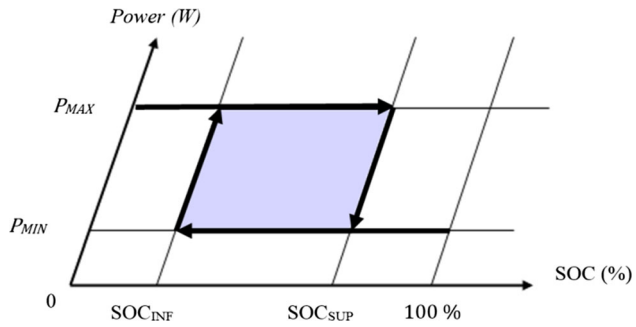

Fig. 15 Hysteresis power management diagram

The purpose is to keep SOC perpetually operating within these two limits regardless of the power flow direction through the inverter (feeding/recovering).

To consider the frequency regulation, the reference power sent from PM layer is then to be passed through the frequency control layer before being sent again to the hybrid inverter control system (Fig. 16).

When the MG frequency is between $F_{\min}$ (minimum frequency value) and F_r (regulation frequency value), the controller injects the entire power sent from hysteresis PM layer without adjustment. When the MG frequency exceeds F_r, the inverter starts the regulation by reducing the amount of power to be fed proportionally to frequency deviation. When the MG frequency is beyond $F_{\max}$ (maximum allowed frequency value), the controller disconnects the PV inverter from the MG allowing only DG to take the charge of frequency regulation. This whole technique is depicted in Fig. 17.

4.2 Fuzzy-based PM

In this section, we describe the proposed fuzzy algorithm to manage the power flow in MG targeting some technical and economical purposes. The proposed controller can simultaneously deal with optimal power sharing and frequency stability in MG. FL controller has as inputs the

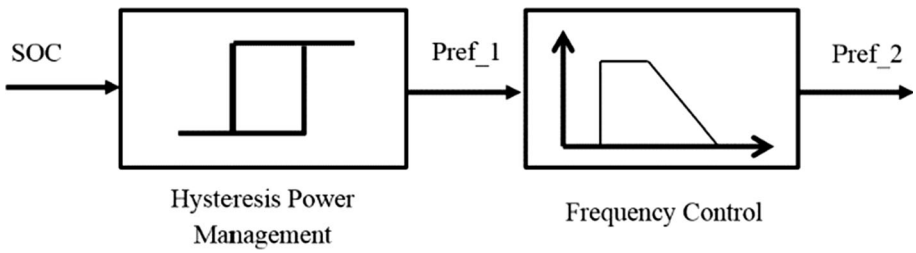

Fig. 16 Hysteresis power management diagram with conventional frequency control

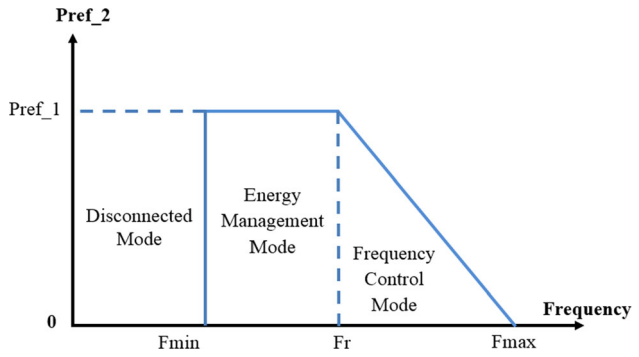

Fig. 17 PV active power control according to frequency regulation

frequency deviation from rated value (50 Hz), solar insolation, and batteries SOC level as shown in Fig. 18.

The frequency deviation gives FL controller an idea about the power balance in MG: Frequency drop means that the power demand is higher than the supplied power, while the frequency rise means an excess of power generation is detected. The insolation, as a second input, provides information about the available PV power in the DC link. Since the ambient temperature has less influence on PV generation compared to the insolation, it is excluded from the controller scheme for a simplification reason. To take the ESS operational constraints into consideration, SOC is included as a third input, keeping it within two limits whatever is the power flow in MG can preserve enough capacity in ESS to react to any sudden ask for power balance adjustment in MG.

Real-time measurement of input variables gives FL controller enough information about the actual operational point in MG, thus allowing it to take appropriate decisions about what amount of power should be exchanged (injected or recovered) with MG (Fig. 19).

According to the number and form of membership functions of inputs/outputs and the implemented logical rules that are figured within the fuzzy surfaces (Fig. 20), FL controller acts, in real time, upon the power exchanged between MG and the hybrid system to achieve the following objectives:

- Favoring the use of PV power instead of DG power when feeding load or charging batteries.
- Injecting more power to MG when the frequency drops and absorbing it when the frequency increases.
- Keeping batteries SOC operating within two predefined control limits.
- Favoring frequency regulation over power dispatching when managing the power in MG.

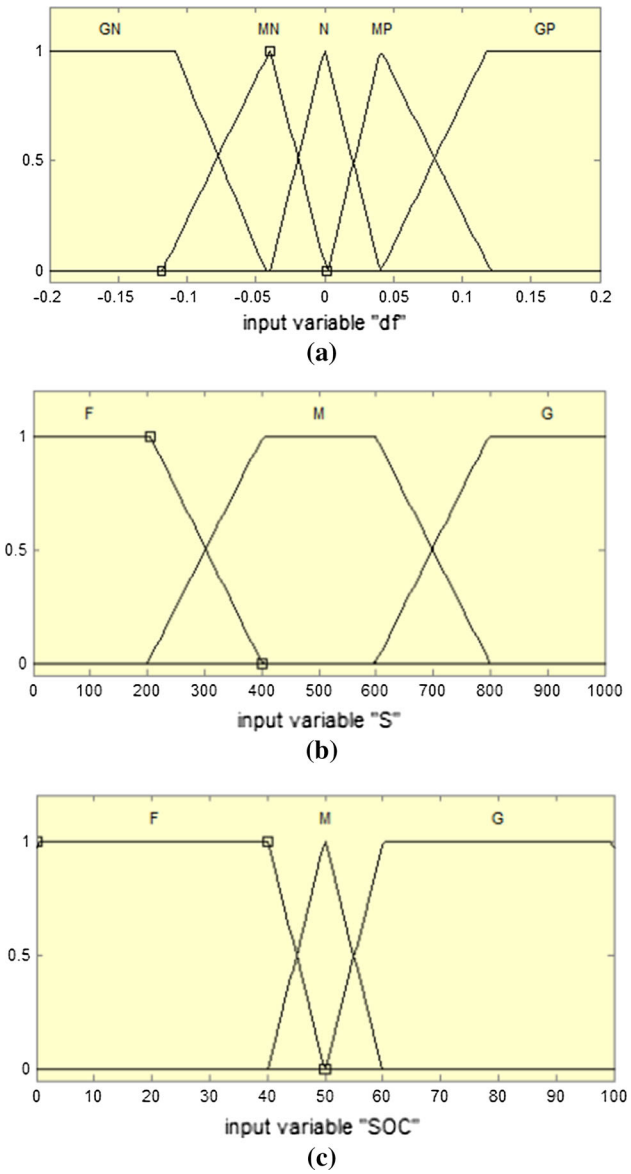

Fig. 18 Fuzzy membership functions of inputs

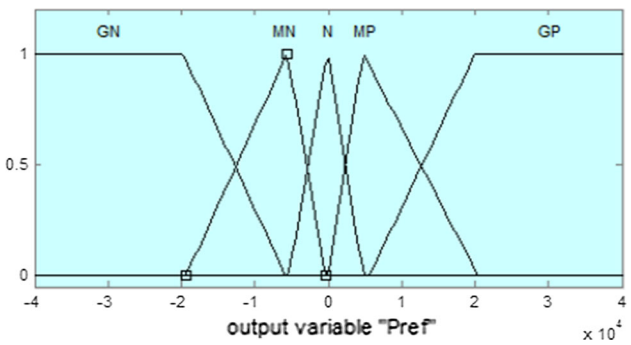

Fig. 19 Fuzzy membership functions of output: exchanged power (Pref)

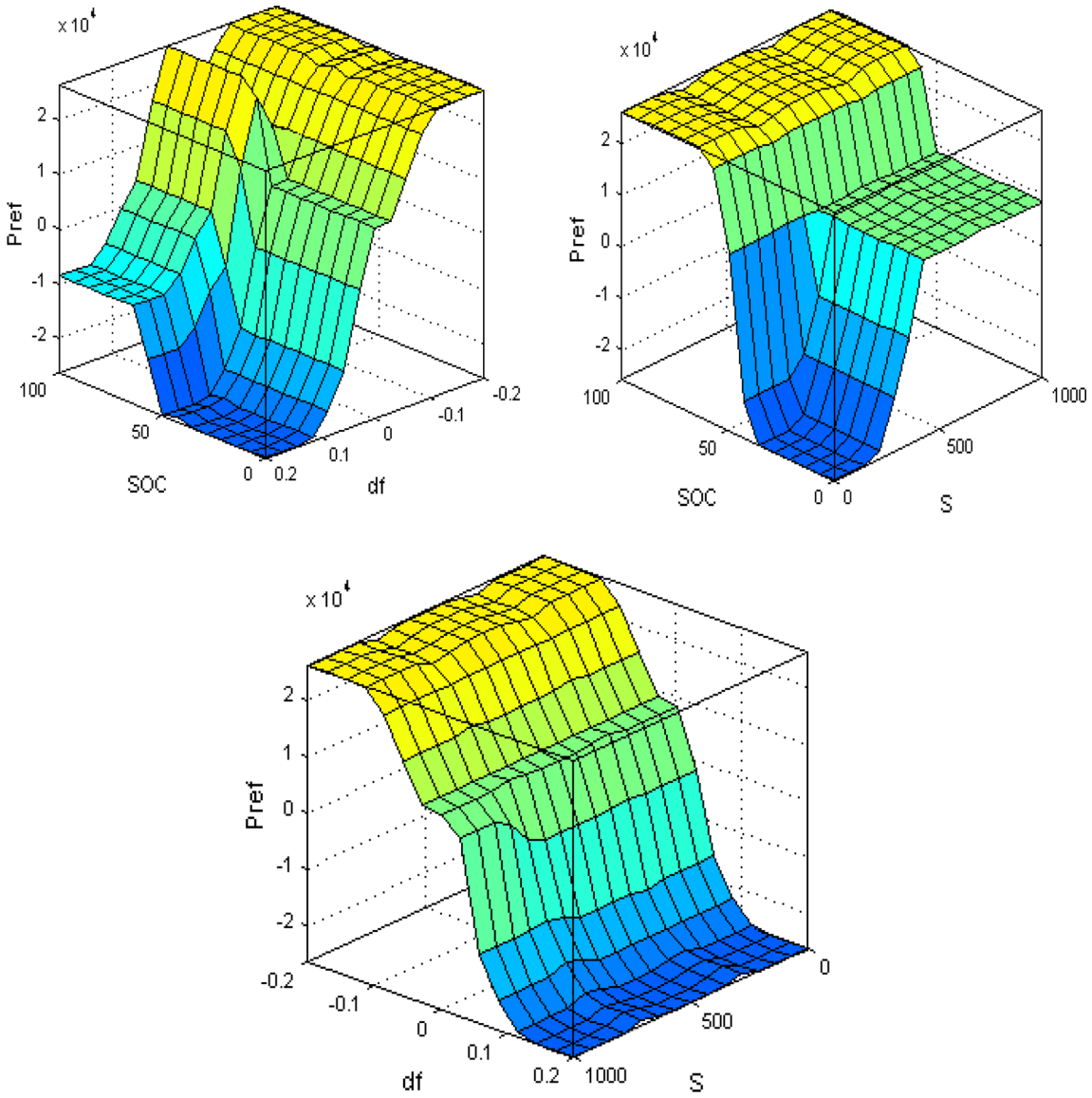

Fig. 20 Fuzzy surfaces that cover all implemented rules

5 Results and discussion

This section presents the simulation results for an off-grid MG with the proposed control techniques using Matlab/Simulink environment. DG, PV, and ESS parameters are cited in Tables 1, 2, and 3, respectively. The power converter parameters are cited in Table 4.

Weather conditions in terms of solar irradiation and temperature are presented in Figs. 21 and 22, respectively. The insolation is a real profile taken in July 9, 2006, in Tamanrasset town (Southern Algeria), and it comprises a deep declining in insolation at nearly 11:15 for less than 1 h due to a cloud movement, which is going to provoke a sudden drop in PV generation. This is considered as an appropriate case to test the robustness of the proposed controller against higher power unbalance in MG between power generation and consumption. Figure 23 shows the chosen load profile which is the residential active power demand of the same town scaled down to 1000.

The first test has been performed using hysteresis PM, and its parameters are cited in Table 5.

In hysteresis PM, the only required feedback signal is SOC measurement, and then the controller manages the power between the energy producers and consumers according to this feedback through the hybrid inverter. SOC is kept inside the optimal zone whatever is the power flow in MG. Supplied PV power feedback is not required since it can be simply estimated through SOC evolution thanks to ESS DC-coupled topology. PV power can be fed directly to MG or stored in ESS according to the power

Table 4 Power converters parameters

Power converter	Parameters	Values
PV DC/DC	Inductance (H)	0.015
	Capacitor (mF)	24
	Input MPPT voltage (V)	280–400
	Output MPPT voltage (V)	500–800
	Rated power (kW)	45
	Switching device	IGBT/Diode
	PWM switching frequency (kHz)	10
ESS DC/DC	Inductance (H)	0.025
	Capacitor (common capacitor with PV DC/DC) (mF)	24
	Input nominal voltage (V)	360
	Output nominal voltage (V)	700
	Rated power (kW)	30
	Switching device	IGBT/Diode
Hybrid DC/AC	PWM switching frequency (kHz)	10
	Rated DC voltage (V)	700
	Rated AC voltage (ph-n) (V)	230
	Rated power (VA)	80
	Switching device	IGBT/Diode
	PWM switching frequency (kHz)	10
	Filter inductance (mH)	5
	Filter capacitor (μF)	600

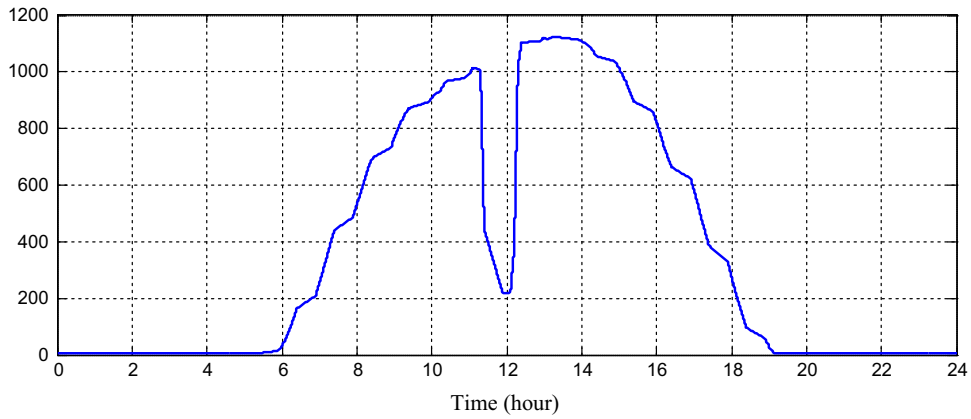

Fig. 21 Solar irradiation variation (W/m^2)

demand and the inverter set point control. Despite its simplicity, hysteresis PM is not designed to maximize the use of PV power. On the other hand, the balance between power generation and consumption in MG is the charge of DG (Fig. 24). Consumed DG energy during the testing day with hysteresis PM is 692,100 kWh.

Since it requires a real-time measurement of insolation, fuzzy PM controller can maximize, as much as possible, the use of PV power when feeding load. SOC, as a second feedback, is necessary for an optimal operation of ESS. Fuzzy rules focus on operating ESS between 50 and 90% as a tolerable operational zone. Contrary to hysteresis PM, FL MP can indirectly follow the power balance in MG using the frequency deviation as feedback. However, the difference between inverter power and load power stills the charge of DG (Fig. 25). In simulation, diesel energy is 608,100 kWh using fuzzy PM.

Figure 26 presents the DC bus regulation for both strategies. With small rapid fluctuations caused by the exchanged power between MG and the inverter, DC voltage is well controlled which means a good balance is satisfied between fed PV/ESS power and the injected/recovered inverter power. In fuzzy PM, the DC voltage regulation is soft due to the smooth power profile in which the hybrid inverter is operated with (Fig. 27).

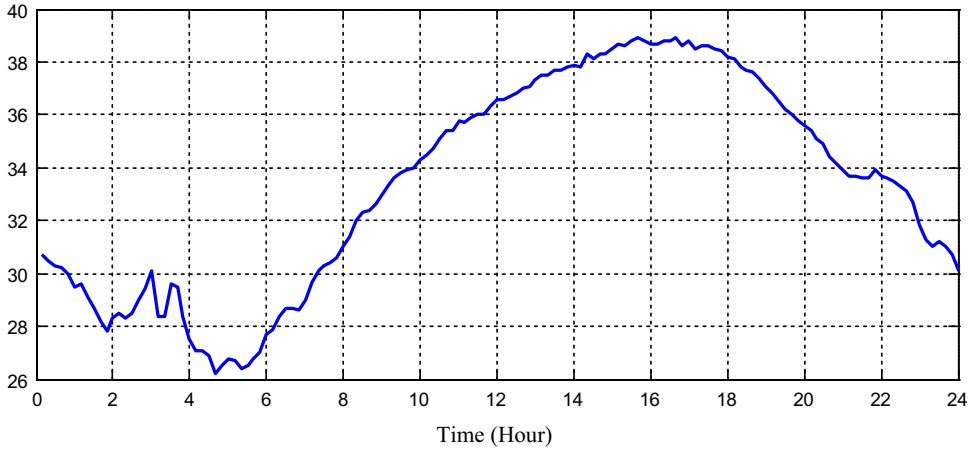

Fig. 22 Temperature variation (°C)

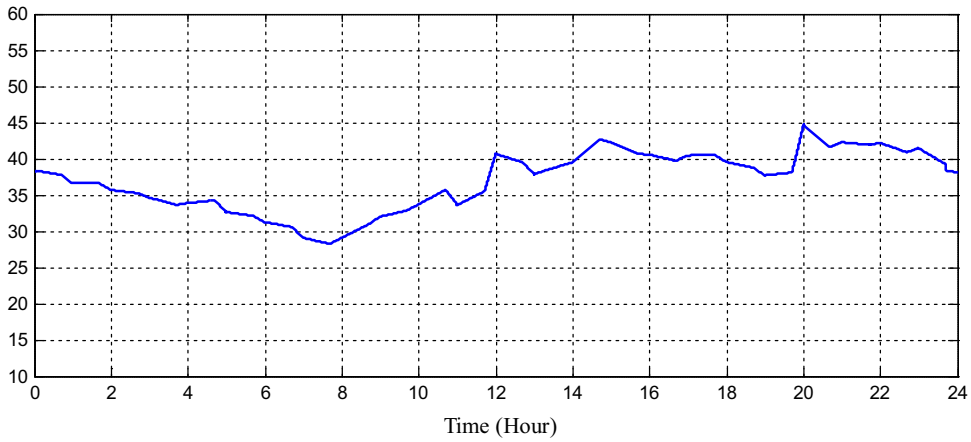

Fig. 23 Load power variation (kW)

Table 5 Hysteresis management parameters

Parameters	Values
Inverter superior power (kW)	25
Inverter inferior power (kW)	− 5
Maximum allowed SOC limit (%)	80
Minimum allowed SOC limit (%)	20
Frequency regulation F_r (Hz)	50.2
Maximum allowed frequency (Hz)	50.5
Minimum allowed frequency (Hz)	49.5

The MG AC voltage quality in the case of fuzzy-controlled inverter (Fig. 28) is slightly better than hysteresis-controlled inverter (Fig. 29). However, THD levels of the AC voltage using both strategies are acceptable.

Despite that a conventional frequency control is provided, frequency deviation when hysteresis PM is applied (Fig. 30) is significant compared to fuzzy PM (Fig. 31), and this is due to the fact that fast changing in the inverter set points with hysteresis PM disturb temporally the MG power balance (black circles). Moreover, PV generation fluctuations (red circles) have also an additional effect, and in fuzzy PM, implemented rules take into consideration the frequency deviation when exchanging power with MG. PV fluctuations in this case are absorbed by ESS, and consequently, fuzzy controller gives priority to frequency control over maximizing PV power, supervising simultaneously SOC evolution.

The main contribution in this study is summarized on the fact that the proposed fuzzy PM can take different time scales tasks in one control action, it is able to control frequency and DC voltage unbalances in terms of seconds, ESS SOC evolution in terms of minutes and the PV maximization in terms of hours. Usually, this can be performed using separate controllers within different layers. The proposed fuzzy-based controller reduces the DG fuel consumption by more than 12% compared to classical hysteresis management control.

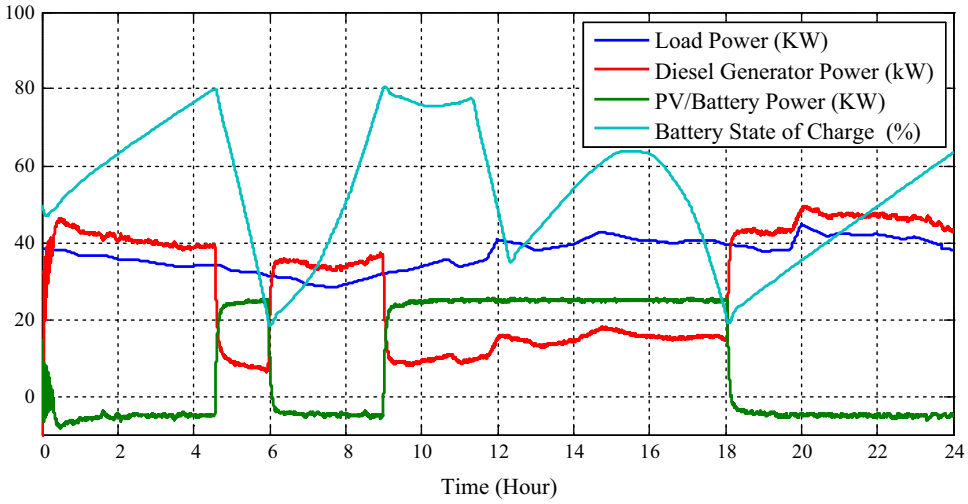

Fig. 24 Power dispatching and battery SOC variation with hysteresis management

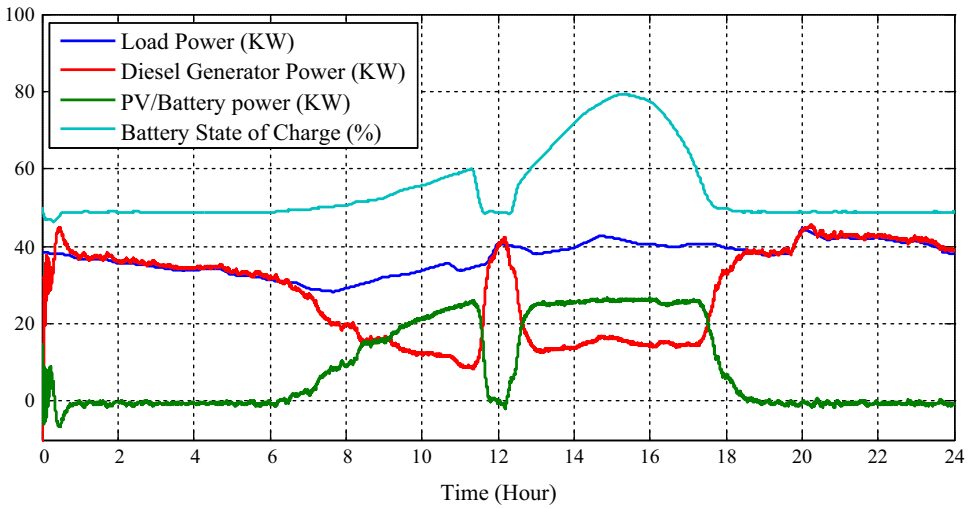

Fig. 25 Powers dispatching and battery SOC variation with fuzzy management

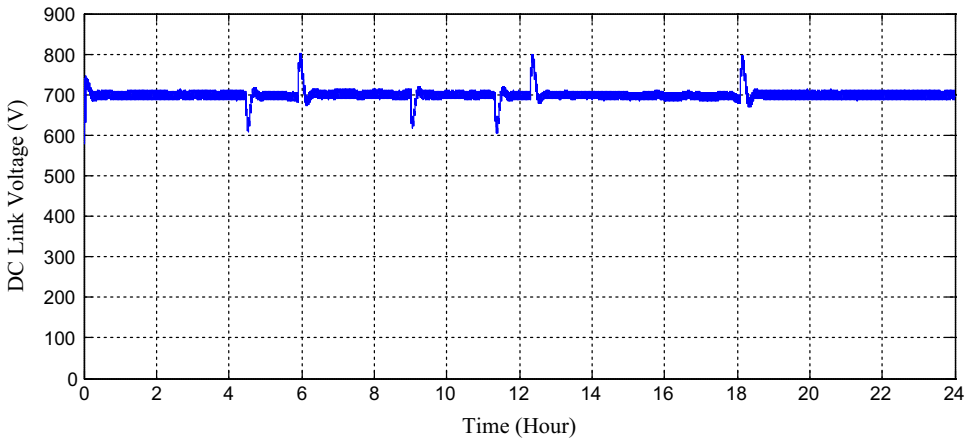

Fig. 26 DC bus voltage variation with hysteresis

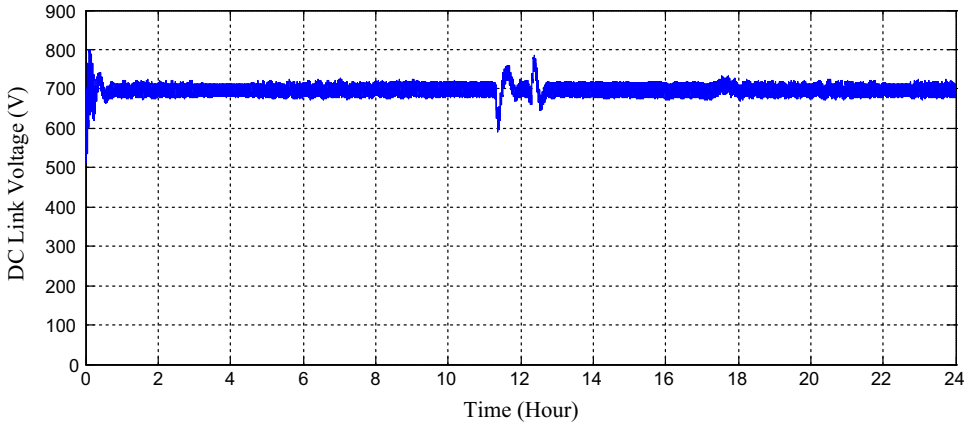

Fig. 27 DC bus voltage variation with fuzzy PM

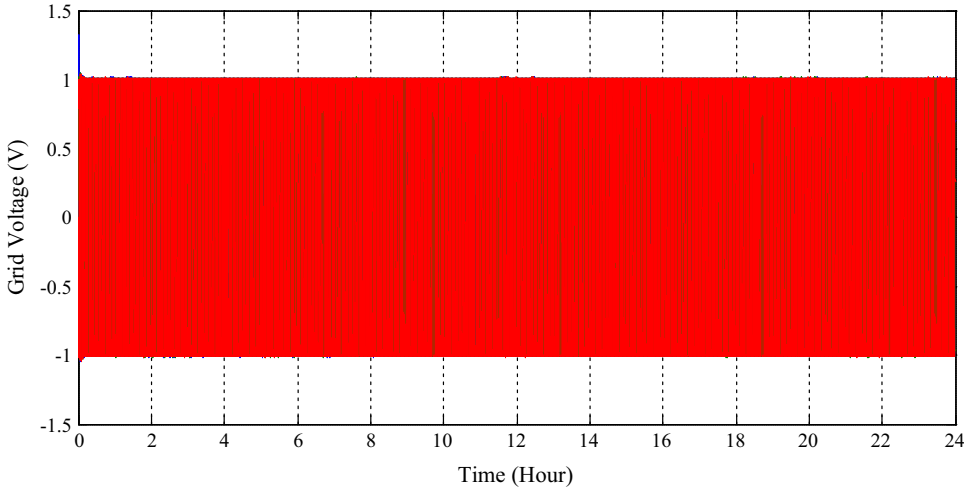

(a)

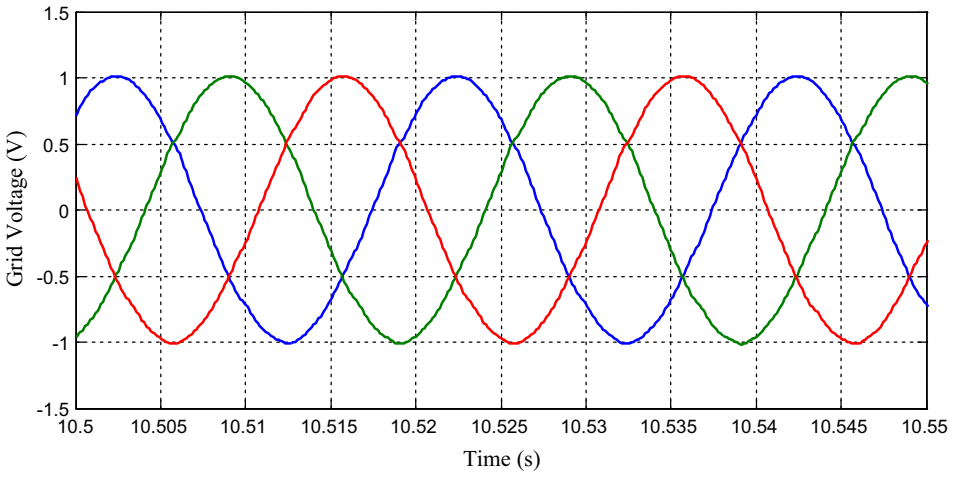

(b)

Fig. 28 **a** AC voltage (pu) fed with fuzzy PM, **b** zoom-in [10.5 s; 10.55 s])

6 Conclusion

This work proposed a new PM for DG, PV, and ESS-based hybrid MG using Mamdani FL technique. The developed controller aims to accomplish several tasks acting only on the hybrid inverter. It optimizes the power flux in MG maximizing the use of PV power when feeding load and operating efficiently ESS. Transient power unbalances in MG, which are usually translated to frequency deviations, are also corrected. The hybrid inverter injects more power

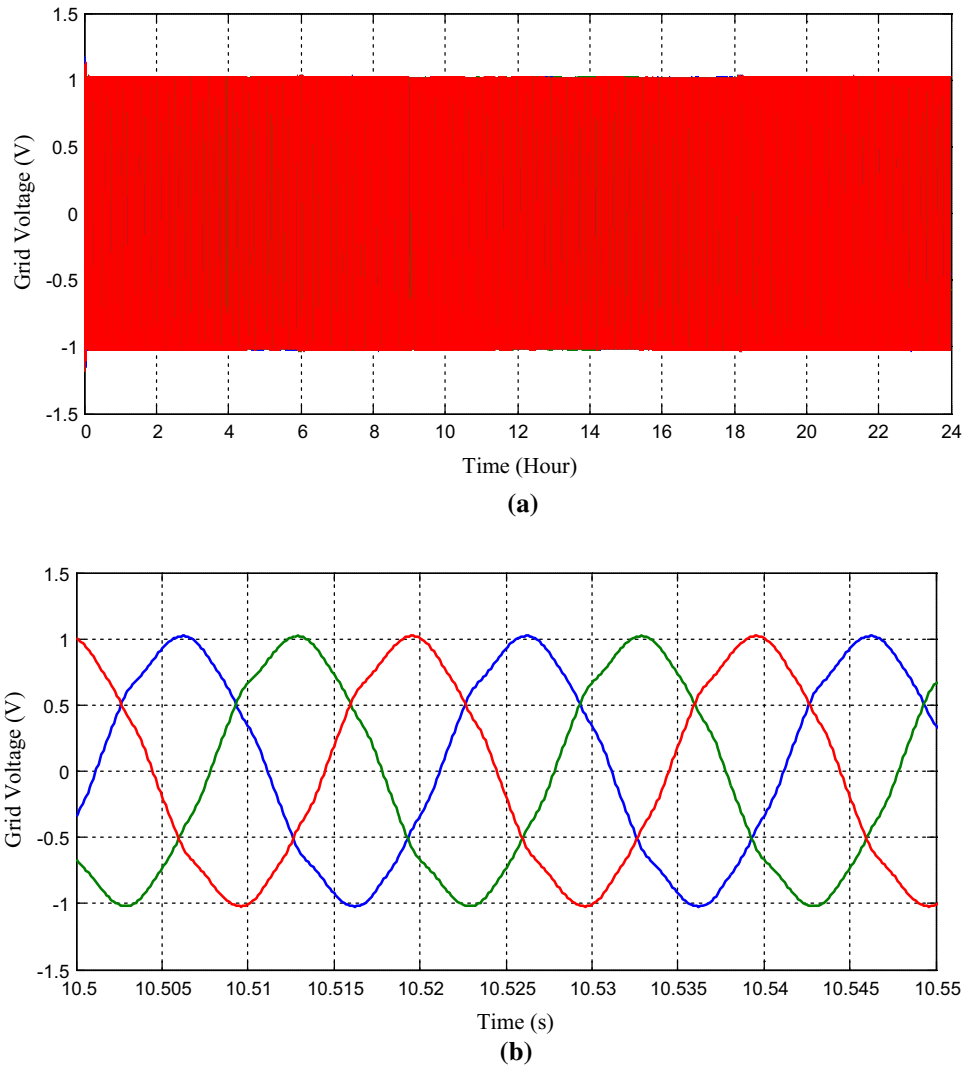

Fig. 29 **a** AC voltage (pu) fed with hysteresis PM, **b** zoom-in [10.5 s; 10.55 s])

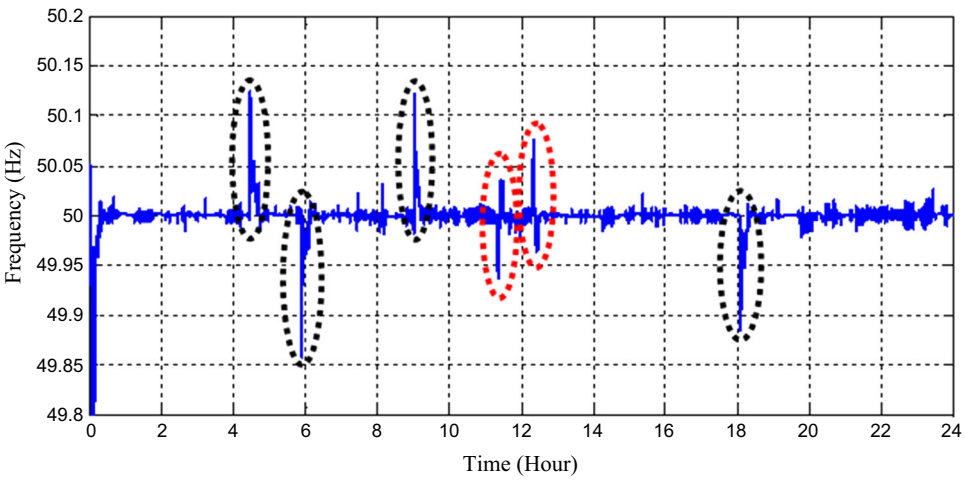

Fig. 30 MG frequency with hysteresis PM

to MG when a frequency drop is detected and recovers it when a frequency rise is detected, in contrast to the classical hysteresis management with a conventional frequency control. Comparative simulation results prove the superiority of the fuzzy controller regarding to the DG fuel economy and MG dynamic stability. The proposed fuzzy-

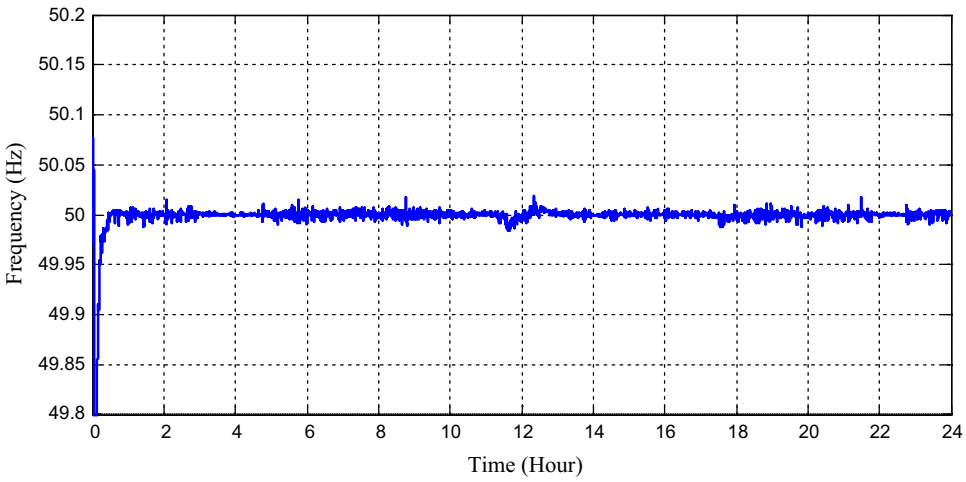

Fig. 31 MG frequency with fuzzy PM

based controller reduces the DG fuel consumption by more than 12% compared to classical hysteresis management control. Moreover, the proposed controller performs well regarding the conventional frequency regulation which is widely used in MGs. As perspective works, the fuzzy controller is to be reconfigured including AC voltage control in MG as an additional feature. With such new pattern, the controller will be able to avoid local over-voltage at the common coupled point while feeding active power which is a typical problem in of low voltage grids. This is feasible by adjusting the reactive power exchange between the hybrid inverter and MG simultaneously with active power feed.

Compliance with ethical standards

Conflict of interest The authors declare that they have no known competing financial interests or personal relationships that could have appeared to influence the work reported in this paper.

References

1. Zhang D, Shah N, Papageorgiou LG (2013) Efficient energy consumption and operation management in a smart building with microgrid. Energy Convers Manag 74:209–222
2. Rossi I, Banta L, Cuneo A, Ferrari ML, Traverso AN, Traverso A (2016) Real-time management solutions for a smart polygeneration microgrid. Energy Convers Manag 112:11–20
3. Zhang L, Gari N, Hmurcik LV (2014) Energy management in a microgrid with distributed energy resources. Energy Convers Manag 78:297–305
4. Hernández ACL, Meng L, Aldana NLD, Graells M, Quintero JCV, Guerrero JM (2017) Online energy management systems for microgrids: experimental validation and assessment framework. IEEE Trans Power Electron 33:2201–2215
5. Hernández ACL, Aldana NLD, Savaghebi M, Quintero JCV, Guerrero JM (2016) Optimal Power Scheduling for an islanded hybrid microgrid. In: Proceedings of 2016 8th international power electronics and motion control conference—ECCE Asia (IPEMC 2016-ECCE Asia)
6. Parvizi-Mosaed M, Farmani F, Anvari-Moghaddam A (2013) Optimal energy management of a micro-grid with renewable energy resources and demand response. J Renew Sustain Energy 5:053148
7. Piagi P, Lasseter RH (2006) Autonomous control of microgrids. In: IEEE PES meeting, Montreal, June 2006
8. Ma Y, Yang P, Wang Y, Zhou S, He P (2014) Frequency control of Islanded microgrid based on wind-PV-diesel-battery hybrid energy sources. In: 17th international conference on electrical machines and systems (ICEMS), Hangzhou, China, 22–25 Oct 2014
9. Habib M, Ladjici AA, Khoucha F (2015) Frequency control in off-grid hybrid diesel/PV/battery power system. In: 4th international conference on electrical engineering. University of Boumerdes, Algeria, 13–15 Dec 2015
10. Oureilidis KO, Bakirtzis EA, Demoulias CS (2016) Frequency-based control of islanded microgrid with renewable energy sources and energy storage. J Mod Power Syst Clean Energy 4(1):54–62
11. Datta MS, Yona T, Funabashi A, Chul-Hwan Kim T (2011) A frequency-control approach by photovoltaic generator in a PV–diesel hybrid power system. IEEE Trans Energy Convers 26:559–571
12. Singh S, Singh SK, Chanana S, Singh YP (2014) Frequency regulation of an isolated hybrid power system with battery energy storage system. In: Power and energy systems conference: towards sustainable energy, 2014
13. Mi Y, Fu Y, Zhao JB, Wang P (2013) The novel frequency control method for PV-diesel hybrid system. In: 10th IEEE international conference on control and automation (ICCA), 12–14 June 2013
14. Tiar M, Betka A, Drid S, Abdeddaim S, Becherif M, Tabandjat A (2017) Optimal energy control of a PV-fuel cell hybrid system. Int J Hydrog Energy 42(2):1456–1465
15. Han Y, Zhang G, Li Q, You Z, Chen W, Liu H (2018) Hierarchical energy management for PV/hydrogen/battery island DC microgrid. Int J Hydrog Energy. https://doi.org/10.1016/j.ijhydene.2018.08.135
16. Ou K, Yuan WW, Choi M, Yang S, Jung S, Kim YB (2018) Optimized power management based on adaptive-PMP algorithm for a stationary PEM fuel cell/battery hybrid system. J Hydrog Energy 43:15433–15444

17. Tabanjat A, Becherif M, Hissel D, Ramadan HS (2018) Energy management hypothesis for hybrid power system of H2/WT/PV/GMT via AI techniques. Int J Hydrog Energy 43(6):3527–3541
18. Hosseini H, Tousi B, Razmjooy N (2014) Application of fuzzy subtractive clustering for optimal transient performance of automatic generation control in restructured power system. J Intell Fuzzy Syst 26(3):1155–1166
19. Razmjooy N, Mehdi R, Noradin G (2017) Imperialist competitive algorithm-based optimization of neuro-fuzzy system parameters for automatic red-eye removal. Int J Fuzzy Syst 19(4):1144–1156
20. Payman M, Razmjooy N, Mousavi BS (2014) Robust potato color image segmentation using adaptive fuzzy inference system. Iran J Fuzzy Syst 11(6):47–65
21. Habib M, Khoucha F (2014) On line energy management strategies for fuel cell/battery electric vehicle: from rules logic to fuzzy logic strategy. In: 2nd international conference on electrical engineering and control applications, Constantine, Algeria, 18–20 Nov 2014
22. Kermadi M, Berkouk A (2017) Artificial intelligence-based maximum power point tracking controllers for Photovoltaic systems: comparative study. Renew Sustain Energy Rev 69:369–386
23. Harrag A, Messalti S (2018) Adaptive GA-based reconfiguration of photovoltaic array combating partial shading conditions. Neural Comput & Applic 30(4):1145–1170
24. Kyriakarakos G, Dounis AI, Arvanitis KG, Papadakis G (2012) A fuzzy logic energy management system for polygeneration microgrids. Renew Energy 41:315–327
25. Datta M, Senjyu T, Yona A, Funabashi T (2011) A fuzzy based method for leveling output power fluctuations of photovoltaic-diesel hybrid power system. Renew Energy 36:1693–1703
26. Roumila Z, Rekioua D, Rekioua T (2017) Energy management based fuzzy logic controller of hybrid system wind/photovoltaic/diesel with storage battery. Int J Hydrog Energy 42(30):19525–19535
27. Papathanassiou SA, Papadopoulos MP (2001) Dynamic characteristics of autonomous wind-diesel systems. Renew Energy 23:293–311
28. Tremblay O, Dessaint LA, Dekkiche A (2007) A generic battery model for the dynamic simulation of hybrid electric vehicles. In: Proceedings of the 2007 IEEE vehicle power and propulsion conference, pp 284–289
29. Long B, Jeong TW, Lee JD, Jung YC, Chong KT (2015) Energy management of a hybrid AC–DC micro-grid based on a battery testing system. Energies 8:1181–1194